

A Superconducting Detector Endstation for High-Resolution Energy- Dispersive SR-XRF

*S. Friedrich, O. Drury, T. Niedermayr, M.F. Cunningham,
M.L. van den Berg, J.N. Ullom, A. Loshak, S.P. Cramer,
J.D. Batteux, E. See, M. Frank, and S.E. Labov*

This article was submitted to
7th international Conference on Synchrotron Radiation
Instrumentation 2000, Berlin, Germany, August 21 – 25, 2000

U.S. Department of Energy

Lawrence
Livermore
National
Laboratory

September 15, 2000

DISCLAIMER

This document was prepared as an account of work sponsored by an agency of the United States Government. Neither the United States Government nor the University of California nor any of their employees, makes any warranty, express or implied, or assumes any legal liability or responsibility for the accuracy, completeness, or usefulness of any information, apparatus, product, or process disclosed, or represents that its use would not infringe privately owned rights. Reference herein to any specific commercial product, process, or service by trade name, trademark, manufacturer, or otherwise, does not necessarily constitute or imply its endorsement, recommendation, or favoring by the United States Government or the University of California. The views and opinions of authors expressed herein do not necessarily state or reflect those of the United States Government or the University of California, and shall not be used for advertising or product endorsement purposes.

This is a preprint of a paper intended for publication in a journal or proceedings. Since changes may be made before publication, this preprint is made available with the understanding that it will not be cited or reproduced without the permission of the author.

This report has been reproduced
directly from the best available copy.

Available to DOE and DOE contractors from the
Office of Scientific and Technical Information
P.O. Box 62, Oak Ridge, TN 37831
Prices available from (423) 576-8401
<http://apollo.osti.gov/bridge/>

Available to the public from the
National Technical Information Service
U.S. Department of Commerce
5285 Port Royal Rd.,
Springfield, VA 22161
<http://www.ntis.gov/>

OR

Lawrence Livermore National Laboratory
Technical Information Department's Digital Library
<http://www.llnl.gov/tid/Library.html>

A SUPERCONDUCTING DETECTOR ENDSTATION FOR HIGH-RESOLUTION ENERGY-DISPERSIVE SR-XRF

S. Friedrich^{a,b,*}, O. Drury^a, T. Niedermayr^a, M.F. Cunningham^a, M.L. van den Berg^a, J.N. Ullom^a,

A. Loshak^a, S.P. Cramer^b, J.D. Batteux^a, E. See^a, M. Frank^a, S.E. Labov^a

^aLawrence Livermore National Laboratory, P.O. Box 808, L-418, Livermore CA 94551, USA

^bLawrence Berkeley National Laboratory, MS 6-2100, Berkeley, CA 94720, USA

We have built a two-stage adiabatic demagnetization refrigerator (ADR) to operate cryogenic high-resolution x-ray detectors in synchrotron-based fluorescence applications. The detector is held at the end of a 40 cm cold finger that extends into a UHV sample chamber. The ADR attains a base temperature below 100 mK with about 24 hours hold time below 400 mK, and does not require pumping on the liquid He bath. We will discuss cryostat design and performance.

Keywords: Adiabatic demagnetization refrigerators, low temperature x-ray detectors, superconducting tunnel junctions, x-ray fluorescence

Corresponding author: friedrich1@llnl.gov

Introduction

Cryogenic x-ray detectors have received wide attention during the last decade because they combine the high energy resolution of grating spectrometers with the broadband efficiency of semiconducting energy-dispersive detectors [1]. Cryogenic detectors fall into two groups: Microcalorimeters and superconducting tunnel junctions (STJs). Microcalorimeters measure the x-ray induced temperature rise of a sensitive thermistor, typically a superconducting transition edge sensor [1, 2] or a doped semiconductor [1,3,4]. Microcalorimeters offer a very high energy resolution of 2 to 5 eV FWHM at for photon energies between 2 and 6 keV [2,3,4]. This comes at the expense of a lower maximum count rate around 500 counts/s, because the relaxation of thermal devices back to their equilibrium is intrinsically slow [5]. STJ detectors measure the increase in tunneling current when a photon is absorbed in one of the superconducting electrodes and excites excess charge carriers above the superconducting energy gap. STJ detectors have achieved a slightly poorer resolution between 2 and 12 eV FWHM for 0.05 to 6 keV photons [6,7,8,9]. However, STJ detectors can be operated at more than an order of magnitude higher count rates [10].

High energy resolution combined with high count rate capabilities make STJ detectors attractive for synchrotron-based x-ray fluorescence spectroscopy (SR-XRF). We have developed Nb-Al-AlO_x-Al-Nb STJ detectors and operated them in an adiabatic demagnetization refrigerator (ADR) in synchrotron applications. Our STJ detectors have achieved an energy resolution between 1.7 and 8.9 eV FWHM at 50 eV to 1 keV [7], and they have been successfully operated at count rates above 10,000 counts/s [10]. We have also demonstrated the capabilities of STJ detectors for SR-XRF applications [11, 12].

The area of a single STJ detector is relatively small, typically 0.2 × 0.2 mm². For practical XRF applications, the STJ detector must therefore be placed close to the sample to acquire data with a reasonable count rate. In our previous demonstration experiments, this was achieved by inserting the sample into the cryostat. Some earlier experiments were also affected by residual

front it, since it is not always practical to bake out the Al vacuum vessel which houses our ADR cryostat. Finally, the necessity to pump on the liquid He bath consumed both time and liquid He. We have therefore designed a new two-stage ADR for SR-XRF where the STJ detector is held at the end of a 40 cm long cold finger that can be inserted into a UHV sample chamber at a synchrotron endstation. Here, we discuss the design of this cryostat.

Cryostat Design

Adiabatic demagnetization is a process of magnetic cooling below a liquid He bath temperature through isothermal magnetization and adiabatic demagnetization of a paramagnetic material [13]. Magnetization lowers the entropy of the paramagnet, and the heat of magnetization is carried into the liquid He bath through a closed heat switch. After opening the heat switch, the magnetic field is decreased sufficiently slowly to keep the entropy of the paramagnet constant, thereby lowering its temperature. The base temperature of an ADR typically varies between 30 mK and 1 K, depending on the ordering temperature of the paramagnet used. ADRs are compact, reliable and easy to use.

The cryostat discussed here uses two different paramagnets, with the first stage cooling to a temperature of 1 K and supporting a second stage which cools to a base temperature below 0.1 K (figure 1) [14,5]. The two-stage design allows operation with a bath temperature of 4.2 K and thus does not require pumping on the liquid He bath. The cryostat is designed for a base temperature of 60 mK, and a hold time per magnetization cycle of 24 hours below 400 mK, the maximum operating temperature of our STJs.

The 30 cm diameter cryostat shell with a 7.4 l liquid N₂ and a 9.6 l liquid He tanks is a commercial design by Infrared Laboratories [15]. The liquid He tank has a cylindrical 10 cm cavity to accommodate the ADR magnet with the paramagnets and a magnetic shield. The 77 K and 4.2 K radiation shields use just one layer of Al foil, rather than several layers of superinsulation

that produces a maximum field of 5 T at a current of 23.1 A. It is surrounded by a Vanadium Permendur magnetic shield with 14.5 mm wall thickness to prevent trapping magnetic flux in the superconducting detector. Although Vanadium Permendur saturates at a magnetic field of 4 T, the field outside the cryostat never exceeds 0.02 T during magnetization, and is orders of magnitude lower after demagnetization at the position of the detector at the end of the cold finger.

To reduce the heat load into the liquid He tank, the current leads to the ADR use high-temperature superconducting BSCCO leads between the liquid N₂ and liquid He cooled stages. They are fabricated by Euris Technologies [16], and have a current rating of at least 25 A at B = 0 and temperatures below 77 K. They are not driven normal during magnetization. However, since the top of the stainless steel liquid He tank can be at temperatures up to 15 K for low liquid He levels, we have to heat sink the low temperature end of the BSCCO leads with an Au-plated oxygen-free high conductivity (OFHC) Cu strap attached to the 4.2 K portion of the He tank. This ensures that the NbTi leads to the ADR magnet always remain superconducting.

We operate both paramagnets with a single magnet and a single heat switch (figure 1). The first stage is cooled by a 143 g single crystal of gadolinium gallium garnet Gd₃Ga₅O₁₂ (GGG). GGG is an attractive material for a guard stage to reduce the heat load into the cold stage because of its ordering temperature around 1 K, its high heat capacity and its high thermal conductivity [14]. The cold stage (0.1 K stage) uses a 63 g homegrown salt pill of Fe(NH₄)(SO₄)₂ · 12 H₂O, commonly known as FAA for Ferric Ammonium Alum. FAA is a poor thermal conductor and also corrodes Cu, requiring growth of the FAA salt pill from an aqueous solution onto a skeleton of solid Au wires, which are silver-soldered to an OFHC Cu post connecting to the cold stage [17]. Furthermore, FAA dehydrates at temperatures above 40 °C thereby losing its paramagnetic properties, and is therefore sealed inside a thin stainless steel can. Since a cryostat with an FAA salt pill cannot be baked out, it is assembled in a clean room wearing latex gloves and using ultrasonically cleaned parts to make it as close to UHV compatible as possible. Both stages are

N (cf. figure 1). Since Kevlar lengthens over time and with thermal cycles, we have cooled each suspension at least four times to 77 K before re-tensioning them and installing them in the cryostat.

We have designed an electrically controlled heat switch to avoid air leakage at the o-ring sealed feedthroughs often found in conventional mechanical heat switches (figure 2). It uses an over-center-cam locking mechanism activated by two solenoids that toggle a stainless steel spring between two stable positions. This bi-stable heat switch does not require any current through the solenoids to keep it closed, and the only heat load into the liquid He bath is due to the 200 ms 1.5 A current pulse through the 3 _ solenoid to activate the plunger. The large mechanical advantage of the heat switch's locking mechanism provides a force of 2000 N to each of the cold fingers, which can be tuned by adjusting the thickness of the fingers. At present, the thermal conductance through the heat switch is 65 mW/K at 4.2 K, sufficient to cool the cold stages to the bath temperature within 20 minutes after magnetization. This sets the time required for a demagnetization cycle.

The STJ detector is mounted at the end of an OFHC Cu rod that is bolted to the 0.1 K stage at three points for stability and thermal contact. This rod is surrounded by an OFHC Cu radiation shield, which also holds the STJ detector magnet needed to suppress the dc Josephson current for stable STJ operation. All of this is enclosed with a second radiation shield attached to the liquid N₂ cooled stage. The diameter of this outer shield of about 45 mm is sufficiently small to fit through standard gate valves. All of these parts are Au plated to prevent them from oxidation for good thermal contact across interfaces. The clearance between the shields of at least 3 mm is sufficient to ensure that stages do not touch each other during cool down or magnetization, provided that the paramagnets are well aligned in the center of the magnet. There are three thin infrared (IR) blocking windows consisting of 200 Å Al on 1000 Å parylene at the end of the cold finger to prevent room temperature radiation from heating the cold stage and causing IR induced excess noise in the detector. Their size is determined by a trade-off between desired angle of acceptance and tolerable IR photon flux [18].

Results and Discussion

Our two-stage ADR has attained a base temperature of 65 mK using a magnetization field of 4.4 T, which allows temperature controlled operation at temperatures down to 70 mK. In unregulated operation, the cold stage had a hold time of about 24 hours below 400 mK, the maximum operating temperature of our STJ detectors. The initial warm-up rate is low, and the detector stays below 200 mK for about 20 hours. The liquid He hold time is more than two days. The time for a demagnetization cycle is about 45 minutes, yielding a duty cycle for the ADR of more than 95%. It is possible to further increase the hold time by not demagnetizing to zero magnetic field, but just to the value required to reach the desired operating temperature, and then slowly decreasing the field to maintain a constant temperature.

Initial tests with a similar two-stage ADR system at the BESSY II synchrotron have achieved an STJ detector resolution of 21 eV FWHM at a photon energy of 270 eV. The resolution improved to around 10 eV with better IR filtering. This is still less than the resolution of nominally identical STJ detectors mounted in the center of an ADR, rather than at the end of a cold finger within 2 cm of a room temperature sample. This discrepancy may still be due to excess noise caused by IR radiation, or due to insufficient shielding of external magnetic fields. The chamber vacuum during operation was in the 10^{-8} mbar range, and no signs of gas freeze-out on the IR blocking windows have been observed.

In summary, we have built a two-stage ADR to operate cryogenic high-resolution STJ x-ray detectors in synchrotron-based fluorescence applications. The STJ detector is held at a temperature around 0.1 K at the end of a 40 cm cold finger within 2 cm of a room temperature sample. The cryostat hold time is about 24 hours per demagnetization cycle, and the outgassing of the unbaked cryostat is compatible with a chamber pressure in the 10^{-8} mbar range. Details of the cryostat and the detector performance will be discussed in a separate publication.

This work was performed under the auspices of the U.S. Department of Energy by University of California Lawrence Livermore National Laboratory under contract No. W-7405-Eng-48. Funding was provided by the NASA Space Astrophysics Detector Development Program grant NAG 5-4137, the NASA High Energy Astrophysics Supporting Research and Technology Program under interagency agreement W19.121, the NASA Constellation X-Ray Mission Technology Development Program under interagency agreement S-10256G, the NIH grant GM 44380, the DOE Office of Biological and Environmental Research, and the Radiometry Laboratory of the Physikalisch Technische Bundesanstalt, Berlin. In particular, we would like to thank R. Fliegauf, M. Veldkamp and B. Beckhoff for their efforts and feedback.

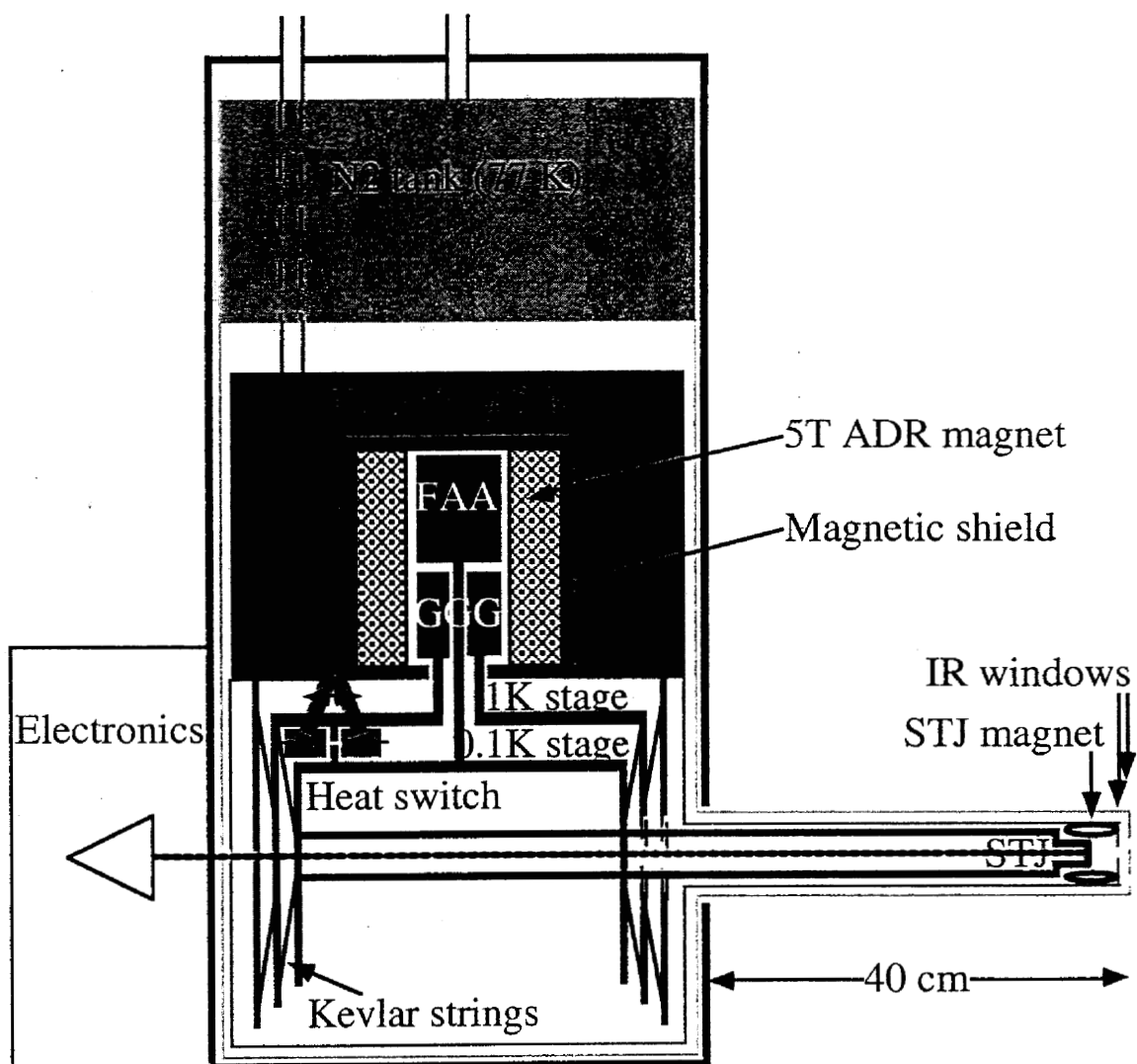
Figure captions:

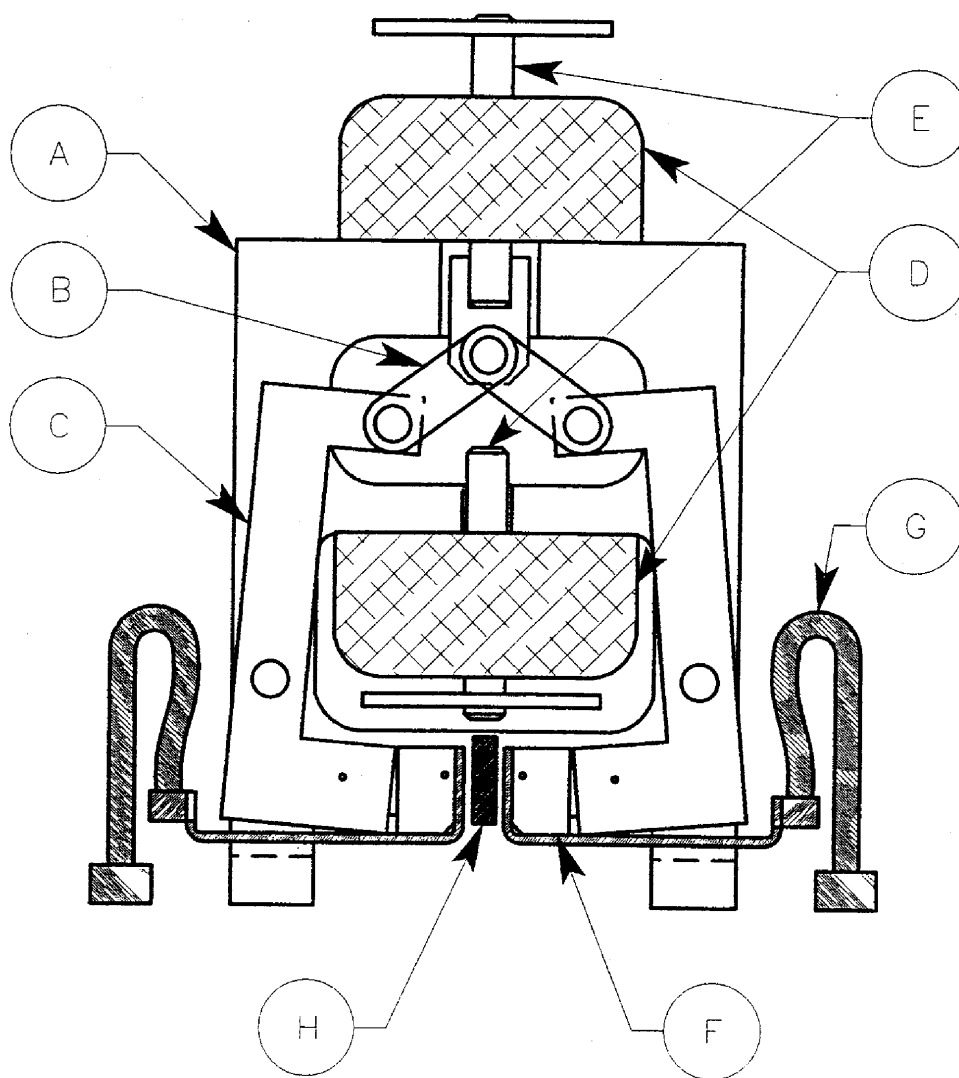
Figure 1: Schematic cross section of the two-stage ADR. The STJ detector operates at a temperature below 0.1 K at the end of a 40 cm cold finger inside a UHV chamber within 2 cm of the sample.

Figure 2: Schematics of the heat switch: A) Stainless steel (SS) frame B) Movable SS links to C) SS springs which rotate about the pivot points (circles). D) Two solenoids (cross-hatched) with plungers (E) for opening (bottom) and closing (top) heat switch. F) Au-plated oxygen-free high-conductivity (OFHC) Cu thermal links (shaded), spring-loaded to pivot at the end of the SS springs (C) to make good thermal contact between the 0.1 K stage and 1 K stage fingers (H) and the liquid He bath through the annealed OFHC Cu-braid (G).

References

- [1] Proceedings of the 8th International Workshop on Low Temperature Detectors (LTD-8), *Nucl. Inst. Meth. A* **444** (2000)
- [2] K.D. Irwin et al., *Nucl. Inst. Meth. A* **444**, 184 (2000)
- [3] E. Silver et al., to be published in *SPIE Proceedings* **4140** (2000)
- [4] A. Alessandrello et al., *Phys. Rev. Lett.* **82**, 513 (1999)
- [5] D.A. Wollman, K.D. Irwin, G.C. Hilton, L.L. Dulcie, D.E. Newbury, J.M. Martinis, *J. Microscopy* **188**, 196 (1997)
- [6] S. Kraft et al., *J. Appl. Phys.* **86**, 7189 (1999)
- [7] S. Friedrich et al., *IEEE Trans. Appl. Supercond.* **9**, 3330 (1999)
- [8] G. Angloher et al., *Nucl. Inst. Meth. A* **444**, 214 (2000)
- [9] D.E. Prober et al., to be published in *SADD Proceedings*, Baltimore (2000)
- [10] M. Frank et al., *Rev. Sci. Inst.* **69**, 25 (1998)
- [11] M. Frank et al., *J. Synchrotron Rad.* **5**, 515 (1998)
- [12] S. Friedrich et al., *J. El. Spectr. and Rel. Phen.*, **101**, 891 (1999)
- [13] See for example O.V. Lounasmaa, "*Experimental Principles and Methods Below 1 K*", Academic Press, London (1974)
- [14] C. Hagmann, P.L. Richards, *Cryogenics* **34**, 221 (1994)
- [15] Infrared Laboratories, Tucson, AZ, USA; <http://www.irlabs.com/>
- [16] EURUS Technologies, Tallahassee, FL, USA; <http://www.teameurus.com>
- [17] C. Hagmann, D.J. Benford, P.L. Richards, *Cryogenics* **34**, 213 (1994)
- [18] S. Friedrich, T. Funk, O. Drury, S.E. Labov, to be published in *SPIE Proceedings* **4140** (2000)





University of California
Lawrence Livermore National Laboratory
Technical Information Department
Livermore, CA 94551

